Spatio-temporal evolution of surface water resources in the Brazilian semi-arid: a case study in the Sertão of Pernambuco

Evolução espaço-temporal dos recursos hídricos superficiais no semiárido brasileiro: um estudo de caso no Sertão de Pernambuco

Geovane de Andrade Silva[1] 🆔 **, Érick Mateus de Souza Freire[2]** 🆔 **, Francisco Gustavo da Silva[1]** 🆔 **,**
José Raliuson Inácio Silva[2] 🆔 **, Antônio Henrique Cardoso do Nascimento[2]** 🆔 **, Elisiane Alba[2]** 🆔 **, Araci Farias Silva[2]** 🆔 **&**
Alan Cézar Bezerra[2] 🆔

[1]Universidade Federal Rural de Pernambuco, Recife, PE, Brasil
[2]Universidade Federal Rural de Pernambuco, Serra Talhada, PE, Brasil

E-mails: geovaneandradep@gmail.com (GAS), erick77mateus@gmail.com (EMSF), francisco.gustavosilva@ufrpe.br (FGS), raliuson.silva@ufrpe.br (JRIS), antonio.cardoso@ufrpe.br (AHCN), elisiane.alba@ufrpe.br (EA), araci.farias@ufrpe.br (AFS), alan.bezerra@ufrpe.br (ACB)

ABSTRACT

The research analyzed the evolution of surface water in Serra Talhada, Brazil, over 31 years using remote sensing data from Google Earth Engine (GEE). It compared the NDWI and MNDWI indices with MapBiomas data to assess water dynamics in semi-arid regions. Accuracy analysis and the kappa index showed good agreement between datasets, while trend testing revealed significant temporal changes during dry and wet seasons. Despite irregular rainfall patterns, the MNDWI index proved more effective in quantifying surface water, highlighting greater water accumulation during the rainy season. Reservoir construction influenced water distribution, but annual water retention varied throughout the study. The results underscore the importance of strategic planning for reservoirs, particularly considering solar exposure, to ensure long-term water availability. The study emphasizes that sustainable water management is essential for environmental and socioeconomic resilience in semi-arid regions, especially in climate variability and increasing demand for water resources.

Keywords: Water; Semiarid; Remote sensing; Google Earth Engine; Temporal trend.

RESUMO

A pesquisa analisou a evolução das águas superficiais em Serra Talhada, Brasil, ao longo de 31 anos, utilizando dados de sensoriamento remoto do Google Earth Engine (GEE). Comparou os índices NDWI e MNDWI com dados do MapBiomas para avaliar a dinâmica da água em regiões semi-áridas. A análise de precisão e o índice kappa mostraram uma boa concordância entre os conjuntos de dados, enquanto o teste de tendências revelou mudanças temporais significativas durante as estações seca e úmida. Apesar dos padrões irregulares de precipitação, o índice MNDWI mostrou-se mais eficaz na quantificação da água superficial, destacando uma maior acumulação de água durante a estação chuvosa. A construção de reservatórios influenciou a distribuição de água, mas a retenção anual de água variou ao longo do estudo. Os resultados ressaltam a importância do planejamento estratégico dos reservatórios, principalmente considerando a exposição solar, para garantir a disponibilidade de água a longo prazo. O estudo enfatiza que a gestão sustentável da água é essencial para a resiliência ambiental e socioeconómica em regiões semi-áridas, especialmente na variabilidade climática e na crescente demanda por recursos hídricos.

Palavras-chave: Água; Semiárido; Sensoriamento remoto; Google Earth Engine; Tendência temporal.

INTRODUCTION

The Brazilian semi-arid region is characterized by high temperatures and irregular rainfall, with a short rainy season and significant inter-annual variability, making the region susceptible to droughts (Pilz et al., 2019). Studies indicate that this region will be one of the most affected by climate change, as increases in local temperatures are likely to exacerbate aridity, thereby increasing the frequency and intensity of droughts and resulting in reduced water resource availability (Marengo et al., 2011; Angelotti et al., 2012). This phenomenon is evident from historical records of drought periods, with the most recent intense drought occurring between 2012 and 2017. Assessing climate change and the dynamics of wetlands and surface water is essential for understanding environmental degradation and its impacts and proposing mitigation measures or policies for adapting to these conditions (Ebrahimi-Khusfi et al., 2020).

Remote sensing has proven to be a powerful tool for monitoring and addressing regional issues. In recent years, there has been a significant increase in the acquisition of remote sensing datasets from various space-based and airborne sensors with different characteristics (Chen et al., 2022). This abundance of data offers continuous regional insights, aiding in understanding natural disasters such as droughts and helping to adopt appropriate mitigation measures. In this context, Google has developed the Google Earth Engine (GEE) platform, a cloud-based storage and processing tool for big data analysis on a global scale (Gorelick et al., 2017; Amani et al., 2020; Chen et al., 2022; Mashala et al., 2023). GEE's accessibility supports regional wetland analysis using earth observation data, encompassing more than 40 years and a petabyte of accessible sensing data (Gxokwe et al., 2022). This extensive historical dataset enables time series analysis essential for identifying random and non-random patterns in variables of interest, facilitating forecasts, and supporting decision-making regarding the rational use and preservation of water resources (Mortatti et al., 2004).

Identifying water surfaces using remote sensing data can be divided into two main categories: single-band and multi-band methods. The single-band method typically involves selecting a band from a multispectral image to extract water information and establishing a threshold to distinguish between water and land (Rundquist et al., 1987; Xu, 2006). However, selecting the threshold value can lead to inaccurate estimates, mixing water information with shadow noise (Xu, 2006). Conversely, the multi-band method leverages differences in reflectance across bands, providing a practical approach for determining water surfaces. This includes indices such as the Normalized Difference Water Index (NDWI) and the Modified Normalized Difference Water Index (MNDWI) (Yu et al., 1998; Xu, 2002, 2006).

Studies in semi-arid areas have utilized products like MODIS in Lake Manyara, Tanzania (Deus & Gloaguen, 2013), and Landsat in an Australian watershed (Tulbure et al., 2016) and in Central Asia (Chen et al., 2022), employing various techniques such as water indices and machine learning. Other studies, such as Silva et al. (1998) and Sousa et al. (2022), have analyzed semi-arid regions in Brazil but did not conduct trend tests. While these studies investigated annual and seasonal changes in water surfaces, there remains a significant gap in temporal trend evaluations in the Brazilian semi-arid region. Additionally, the recent launch of the "Mapbiomas Água" collection by the Mapbiomas project, following the methodology proposed by Souza Junior et al. (2019), provides annual and monthly data but has limitations in specific spatial coverage, such as micro-basins or local reservoirs. Therefore, we propose an evaluation of a semi-arid region of Brazil that can serve as a basis for studies and applications in areas not covered by MapBiomas.

Our primary hypothesis is that surface water in the Serra Talhada region increased from 1990 to 2020. Hence, our objective was to investigate surface water dynamics in the municipality of Serra Talhada over this period. We sought simple and effective methods for identifying surface water using remote sensing products to achieve this. We conducted time trend tests across different segments of the historical series, focusing on the dry and rainy periods, to understand the region's standard behaviors.

CASE STUDY

The study was conducted in Serra Talhada, part of the Caatinga biome. This region is one of the most populated and biodiverse seasonally dry tropical forests (SDTF) globally, and it is characterized by scarce rainfall and high temperatures, typical of the northeastern semi-arid zone (Barros et al., 2021; Araujo et al., 2023). The Caatinga biome, a seasonal dry forest, has xerophytic vegetation adapted to water scarcity, with thorny trees, shrubs, and drought-resistant plants. The climate is semi-arid, hot, and dry (BSw'h'), with annual rainfall of 657 mm and an average annual temperature of 25.8 °C (Alvares et al., 2013; Lins et al., 2018; Costa et al., 2021). Serra Talhada has a territorial extension of approximately 2980 km², located in the Mesoregion of Sertão Pernambucano, at coordinates 07°59'31''S, 38°17'54'' W, and an altitude of 429 m above sea level (Figure 1).

According to the Serviço Público Federal (Brasil, 2017), the region's economy is firmly based on agriculture, with corn cultivation and livestock farming standing out. In addition, sectors such as education, health, transportation, and tourism contribute significantly to the local economy.

MATERIAL AND METHODS

Figure 2 shows the flowchart detailing the stages of the methodology and the methods used in this research.

Database

Rainfall data

The monthly rainfall data was collected from the National Institute of Meteorology (Instituto Nacional de Meteorologia, 2024) from 1990 to 2020. Based on the seasonality of the rainfall (Figura 3A) and da Costa et al. (2021), we considered a dry period from August to November and a rainy period from January to April.

Rodrigues et al. (2022) reported that the driest and wettest years occur due to El Niño and La Niña, respectively. In dry years, the rainy months typically range from November to April, while
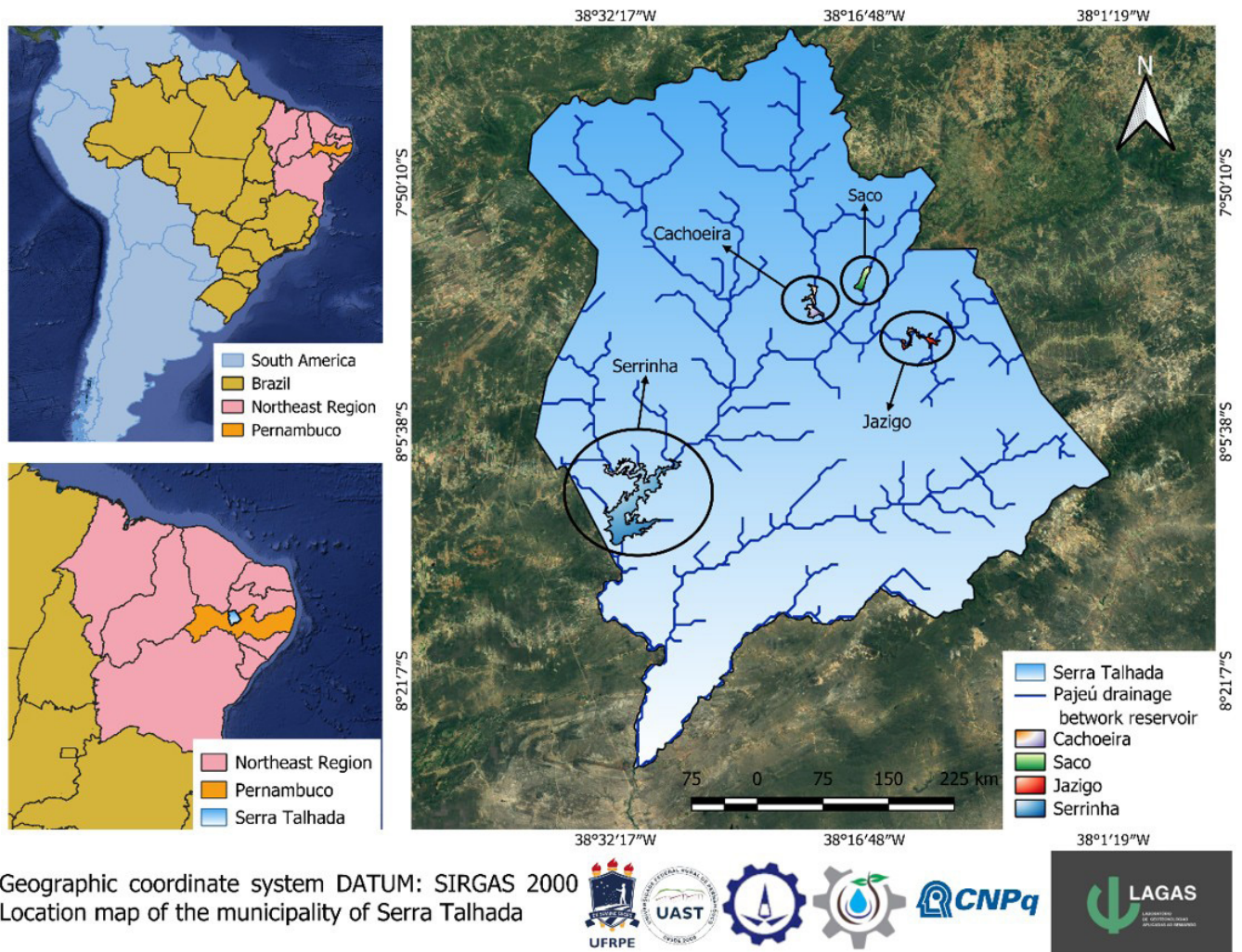
Figure 1. Study area location, drainage network, and reservoirs.

the dry months extend from July to November. In normal years, the rainy season goes from January to May, and the dry season from July to November. In wet years, the rainy season spans from December to May, and the dry season lasts from June to November (Gouveia et al., 2024). Therefore, November is considered a transitional month from dry to rainy.

Considering the annual accumulation (Figure 3B), the average rainfall values were 59.69 mm per year, 31.69 mm in dry and 104.94 mm in the rainy season. Notably, from 2012 to 2017, all periods showed low rainfall accumulation due to drought. In 1999, the rainy season had less rainfall than the dry season, reflecting the irregular rainfall characteristic of the semi-arid region, where rain does not necessarily occur in the expected season.

Water surface indices

To estimate surface water, the following indices were calculated: the Normalized Difference Water Index (NDWI) and the Modified Normalized Difference Water Index (MNDWI).

The NDWI is a mathematical model proposed by McFeeters (1996) and is based on the principle that the Near Infrared (NIR)

is strongly absorbed by water and reflected at the same intensity by terrestrial vegetation and dry soil. This index is calculated using Equation 1:

$$NDWI = \frac{pGreen - pNIR}{pGreen + pNIR} \tag{1}$$

where: pGreen is the radiation reflected in the green band, and pNIR is the radiation reflected in the near-infrared band.

The MNDWI is an improved model proposed by Xu (2006) since the NDWI image is often mixed with accumulated terrestrial noise, especially in the NIR band. The MNDWI is estimated using Equation 2:

$$MNDWI = \frac{pGreen - pSWIR}{pGreen + pSWIR} \tag{2}$$

where: pSWIR is reflected in mid-infrared radiation. This mathematical model ranges from -1 to +1, proposing that values from -1 to 0 are soil and values from 0 to +1 are water, i.e., the interpretation is equal to the NDWI.
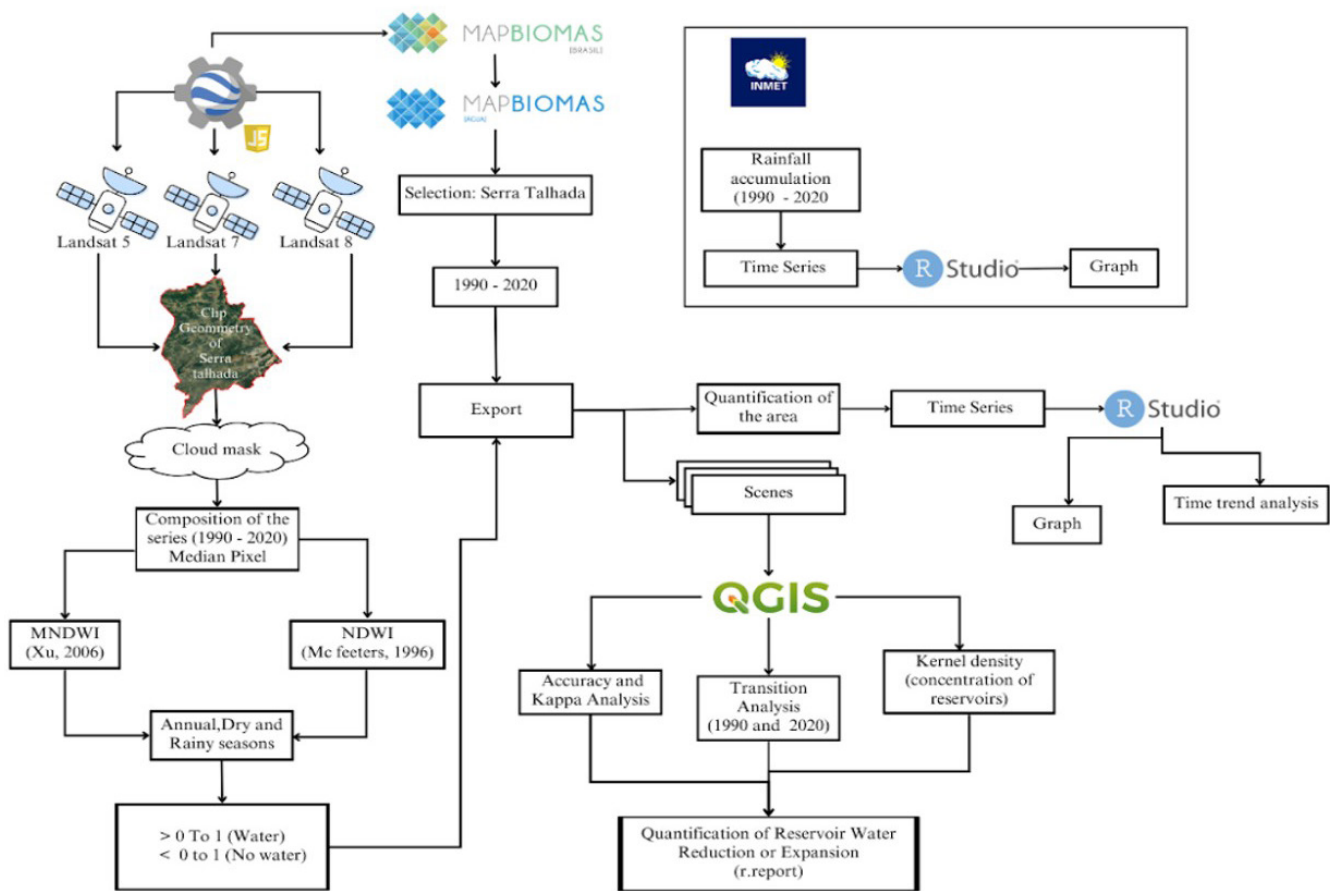
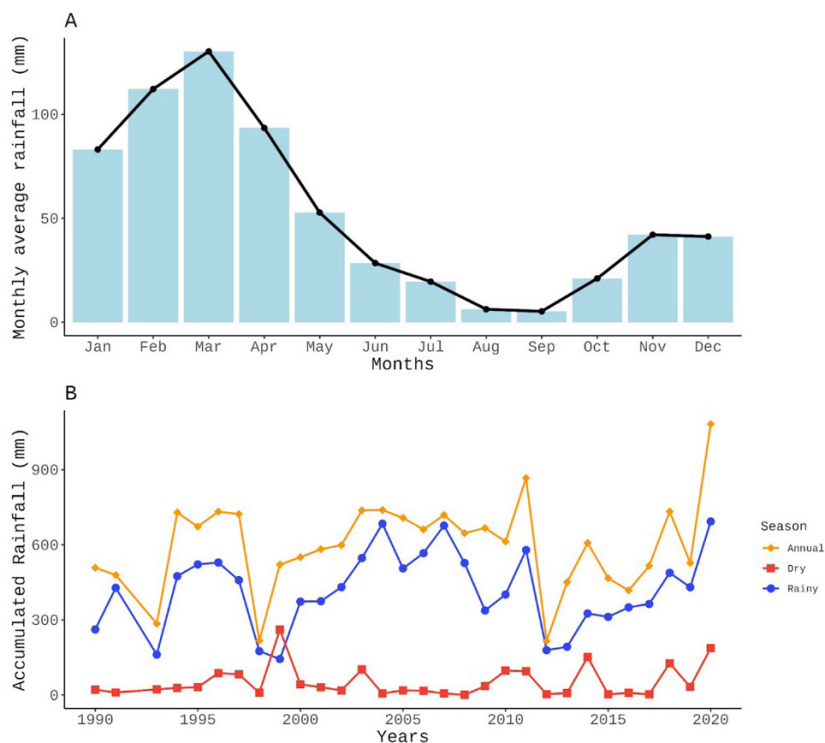**Figure 2.** Flowchart of the work methodology.

Figure 3. Rainfall variability in Serra Talhada: (A) Monthly average accumulated rainfall (mm); (B) Annual and seasonal rainfall accumulation (dry and rainy) in millimeters (mm) from 1990 to 2020.
Source: Instituto Nacional de Meteorologia (2024).

Therefore, we used the NDWI equation to perform annual quantification, while the MNDWI equation was applied for annual measurements and separate analyses during the dry and rainy seasons. In addition, based on the MNDWI, the transition map from 1990 to 2020 and the kernel density map were generated.

MapBiomas

The Mapbiomas collections aim to contribute to developing a fast, reliable, collaborative, and low-cost method for processing large-scale data sets and generating historical time series of annual maps. All data, classification maps, codes, statistics, and other analyses are openly accessible through the platform MapBiomas (2024) The main objective of the MapBiomas Water collection is to provide monthly and annual data on the dynamics of surface water and water bodies throughout the national territory since 1985. The methodology adopted involves selecting images from Landsat versions 5, 7, and 8. Mapping is conducted on a sub-pixel scale using the Mixture Spectral Model (MEM) and empirical classification rules based on fuzzy logic (Souza Junior et al., 2019, 2025).

In this study, data from the MapBiomas Water Collection were used. These data were employed to analyze the time series of water accumulation, create the transition map from 1990 to 2020, and generate the kernel density map.

Images processing

We processed the satellite images on the Google Earth Engine platform, using three orbital satellites of the Landsat 5, 7, and 8 versions, which have a spatial resolution of 30×30 meters and a temporal resolution of 16 days. The period considered in the evaluation was from 01/01/1990 to 31/12/2020. Within the collection of images, we used cloud cover of up to 50% as a criterion, accounting for a total of 1185 images over the 30-year interval. We then reduced the images to the annual level, starting with the median pixel.

To understand the seasonality of the surface water area, we carried out an analysis by dry period - August to November - and rainy period - January to April - in the region, based on the MNDWI, from 1990 to 2020. In the rainy season, 404 images were obtained, while in the dry season, 537 images were obtained. Both periods use up to 60% cloud cover since the rainy period has a more significant presence of clouds and could significantly restrict the availability of images.

We classified the NDWI and MNDWI images based on pixel values. In both images, we classified pixels with values above 0 (> 0) as water and those with values below 0 (< 0) as land surface.

We used it as a threshold for separating water and non-water based on the work of McFeeters (1996) and Xu (2006) studies.

Accuracy and concordance

To assess the capacity of the water indices, we inserted the images classified at an annual level in 2020, both from NDWI and MNDWI, into QGIS, together with a 2020 image from the Water Collection from Mapbiomas. We chose Mapbiomas as a reference because it has an overall accuracy of 84.0% (MapBiomas, 2024), from which we estimated the confusion matrix with the NDWI and MNDWI classifications (Diniz et al., 2021).

The confusion matrix (Table 1) describes the sample classes and the number of pixels that interfere with a good classification due to the confusion caused by similar pixels. Based on the matrix, we determined some metrics, such as the kappa index and accuracy, which express the accuracy of the mapping, according to Ferreira (2022). We used the Semi-Automatic Classification (SCP) plugin developed by Congedo (2021), aimed at a supervised classification of remote sensing images, which provides different tools for downloading, pre-processing, and post-processing images to generate the confusion matrix. Among the tools, one stands out for its analysis of accuracy and Kappa.

The confusion matrix (Table 1) is a fundamental tool for evaluating the performance of binary classification models. The results are categorized into true positives (VP), true negatives (VN), false positives (FP), and false negatives (FN). From this matrix, we calculate metrics such as accuracy, which indicates the proportion of correct classifications (Equation 3), and the Kappa coefficient, which quantifies the degree of agreement between classifications, adjusting for the possibility of random hits (Equation 4). Kappa is considered a more robust measure than accuracy, as it considers both classification hits and errors (Leroux et al., 2018).

$$Accuracy = \frac{Total\ Hits}{Total\ items} \quad (3)$$

$$Kappa = \frac{Pagree - Pchance}{1 - Pchance} \quad (4)$$

Time trend test

The temporal variability of surface water cover in Serra Talhada was assessed by quantifying the water surface area in

Table 1. The confusion matrix for binary classification, where (n) is the number of cases 1.

| | Classification | Reference | | |
		+	−	Σ
Map	+		b	n+
	−	c	d	n−
	Σ	n+	n−	n

images from different periods (annual, dry, and rainy). The data were processed in R (version 4.3.2) using the ggplot2, dgof, trend, and modifiedmk packages (Arnold & Emerson, 2011; Wickham, 2016; Pohlert, 2023; Patakamuri & O'Brien, 2023).

The Mann-Kendall test, as described in studies such as Pandey et al. (2023), is based on the hypothesis that there is no trend over time, while the alternative hypothesis is that there is a trend in the historical series, whether positive or negative. A significance level of α = 0.05 was adopted for all analyses.

Determining changes in water classification areas

To determine the changes in water classification areas over time, we utilized QGIS software version 3.28.4 along with the Semi-Automatic Classification (SCP) plugin, specifically within the "assessing LULC" module of the post-processing tab, as outlined by Congedo (2024). This module facilitates the comparison of two classified images and extracts gains, losses, and overall changes in Land Use and Land Cover (LULC) from 1990 to 2020.

The processing step generates a new raster layer highlighting pixels with classification changes and a CSV file detailing all class transitions. To quantify the reduction or expansion in the areas of the Cachoeira, Saco, and Jazigo reservoirs, located in the northeastern part of the map, and the Serrinha reservoir, located in the southwestern part (Figure 1), in hectares, we used the r.report tool available in GRASS GIS.

Reservoir dynamics

We conducted an additional analysis in Qgis to identify the patterns of surface water reservoirs. We vectorized the images classified based on the MapBiomas indices for 1990 and 2020, removing the vectors of the areas corresponding to non-water. We then extracted the centroids of each vector and applied kernel density estimation, a data visualization technique that uses a color map to represent the density of points in a two-dimensional space (Medeiros & Costa, 2008). This was accomplished using the "heat map" tool available in QGIS.

Silverman (1978) describes that given a sample of data X1, X2, ... Xn from an unknown distribution, the kernel estimate fn(x) for the probability density at point x is given by Equation 5.

$$f_n(x) = \frac{1}{n.h^d} \sum_{i=1}^{n} k\left(\frac{|x - x_i|}{h}\right)$$ (5)

where: fn(x) is the estimated density of the point, n is the total number of points in the data set, h is the width parameter of the kernel, i.e., the radius, which controls the smoothness of the estimate, and influences the scale of the heat map, d is the dimension of the space (usually two-dimensional), and k is the kernel function, x the position of the center of each cell and xi the position of point I from the centroid of each polygon.

This analysis is intuitive as it allows visual identification of areas with higher density through more intense tone or color, indicating a higher concentration of points. On the other hand, lighter colors indicate lower concentration. This technique enables us to assess the increase and decrease in the concentration of the reservoirs over time.

RESULTS

Classification performance with water indices

In Figure 4, it can be observed maps of surface water and non-water classifications based on the NDWI, MNDWI, and MapBiomas values for 2020 in Serra Talhada-PE (Figure 4). These maps highlight the municipality's main reservoirs—Cachoeira, Saco, Jazigo, and Serrinha—as shown on the location map (Figure 1), and indicate regions with a higher presence of small areas of surface water accumulation, which could correspond to regions with small dams.

Overall, the region contains several large reservoirs, such as Serrinha II, in the southwestern part of the study area. Other reservoirs near Serra Talhada, such as the Cachoeira II, Saco, and Jazigo reservoirs, are in the northeast.

We used MapBiomas' image as a reference to analyze the classification capacity of water indices. As previously discussed, the choice of the Mapbiomas reference image was reinforced by the fact that it showed satisfactory classification results in previous analyses. Table 2 presents the results of the accuracy and agreement statistics of the NDWI and MNDWI indices compared with Mapbiomas.

The results suggest that both NDWI and MNDWI classifications exhibit similar performance, with MNDWI showing slightly higher accuracy and kappa metrics values. We used MNDWI to analyze dry and rainy periods.

Temporal trends

The inter-annual variability of the water surface area (hectares) from 1990 to 2020 is shown in Figure 5. In panel 5A,

Table 2. Binary confusion matrix and accuracy metrics for NDWI and MNDWI.

Matrix Error	Reference	Classified	Pixel Sum NDWI	Pixel Sum MNDWI
1	0	0	3266795	3265498
3	0	1	1985	3282
2	1	0	6585	4780
4	1	1	33457	35262
	Overall accuracy [%]		997.410	997.563
	Kappa		0.8852	0.8962
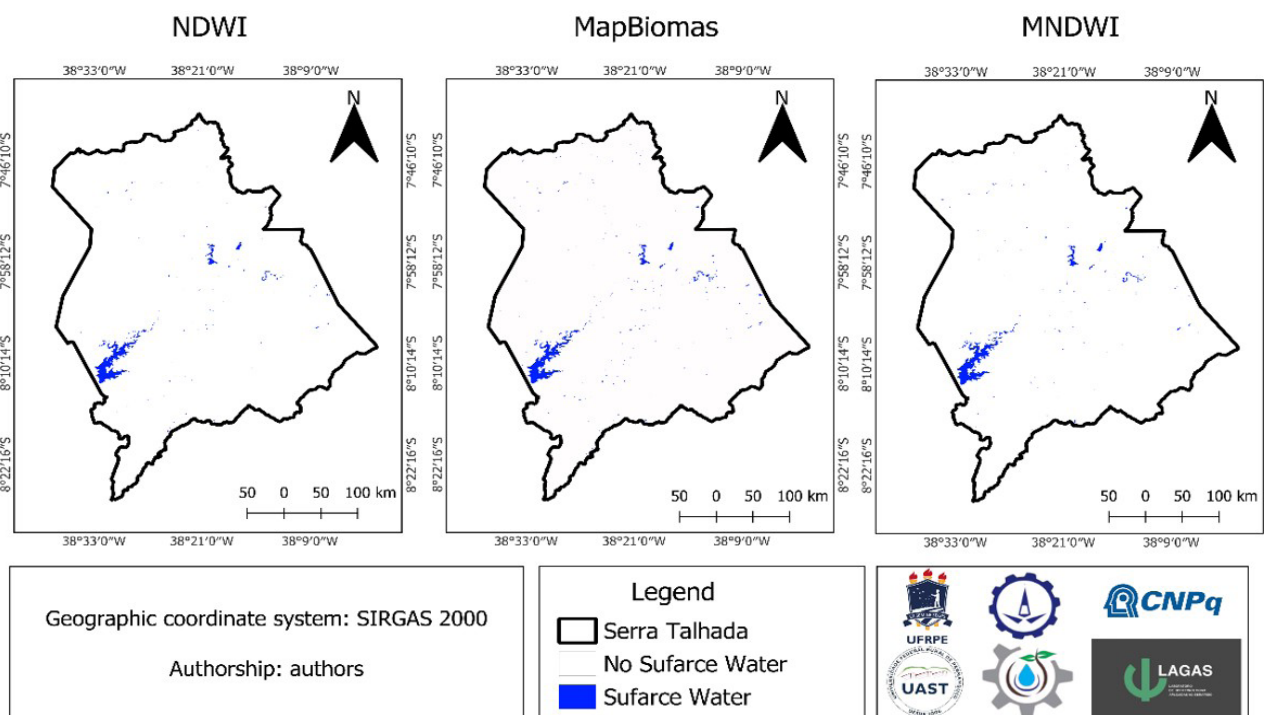
**Figure 4.** NDWI, MapBiomas, and MNDWI water classification in 2020, Municipality of Serra Talhada, PE.

one can observe the values obtained from MapBiomas, MNDWI, and NDWI, while panel 5B presents the areas classified by MNDWI during the dry and rainy seasons. A notable similarity in the behavior of the indices reinforces the consistency of the results, including accuracy and kappa values. The straight lines indicate the trend lines of the historical series.

The MapBiomas results showed a minimum area of 873.65 ha of water in 1993, a maximum of 4,601.85 ha in 2004, and an increasing trend line. The MNDWI results were similar, with a minimum of 601.76 ha in 2017 and a maximum of 4,363.52 ha in 2008, and a rising trend line. The NDWI indicated a significant decrease in the water surface area in 2009, possibly due to contamination or issues with the near-infrared (NIR) product. The minimum value detected by NDWI was 98.4 ha in 2001, and the maximum was 3,576.96 ha in 2006, and an upward trend line.

The results highlight the inter-annual variability of water accumulation, consistent with the precipitation variability (Figure 3). A significant increase was observed in the second half of the 2000s, coinciding with a rainy period between 2004 and 2010 (Figure 3). This increase may also be associated with the completion of the construction of the Serrinha II dam in 1996, which has a water storage of 3,000,000 m³, and other small reservoirs in the municipality.

During the dry season, the MNDWI indicated the lowest quantification of surface water in 1997, accounting for 221.92 per hectare of water, and the maximum value is in 2008, with 4,152.96 ha. In the rainy season, the minimum value recorded was 189.44 hectares in 2014, while the maximum was 5,190.88 hectares in 2008. In both cases, the trend line showed a positive slope.

Notably, surface water variability between periods was observed. For example, in 1992, 282.24 ha of water was quantified
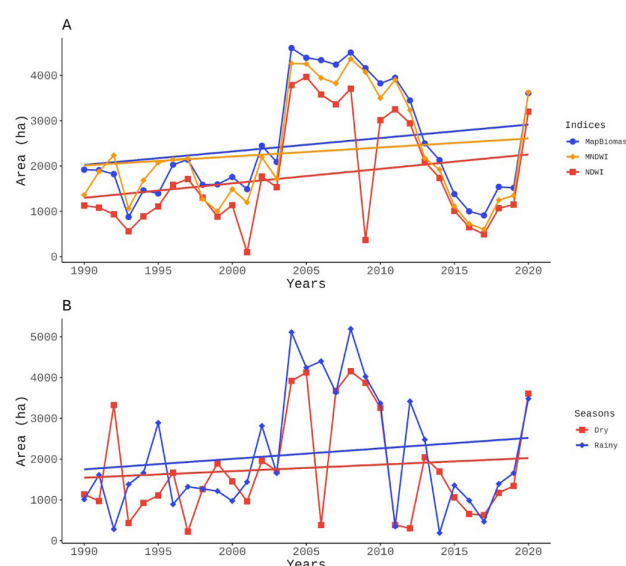
Figure 5. Interannual variability of surface water area (1990-2020) with trend lines: (A) Annual data derived from MapBiomas, MNDWI, and NDWI; (B) Seasonal data (dry and rainy periods) derived from MNDWI. Straight lines represent trend lines.

in the rainy season compared to 3,323.84 ha in the dry season, reflecting the year's climatic irregularity. In 2006, the region had 4,397.92 ha of water in the rainy season and 385.92 ha in the dry season.

To verify the changes between 1990 and 2020, it is observed in Table 3 the time results. Trend test for the NDWI, MNDWI, and MapBiomas indices, both at an annual level and during the

dry and rainy periods. The results indicate convergence between the classification methods, with an upward trend at an annual level and during the rainy season, as evidenced by the positive β values. Conversely, the dry season showed a downward trend (β<0), although all tests showed non-significant values for the temporal trend.

The results indicate that despite the significant increase in surface water impoundment capacity observed between 2004 and 2010 (Figure 5), the temporal trend shows stability. The data also suggests an increase in annual levels during the rainy periods, contrasting with a reduction observed in the dry period. Extreme events are also observed, such as the droughts in 1993 and 2017 and the period of heavy rainfall from 2004 to 2008.

Surface water transition between 1990 and 2020

Although the temporal trend tests indicate stability in the surface water area, we developed an analysis to identify possible changes in the occupation pattern in the study area. Illustrated in Figure 6, the transition of surface water, represented by the MNDWI index and MapBiomas, in the municipality of Serra Talhada - PE from 1990 to 2020. The analysis used the post-processing tool of the SCP plugin in QGIS to check the transition of water and non-water classes based on images from 1990 and 2020. The red color indicates a change from water in 1990 to non-water in 2020, blue indicates areas classified as water in 2020, and green indicates the maintenance of the water classification in both years.

The MNDWI data showed that 703.89 ha of water were converted into non-water areas, while 2,830.95 ha became classified as water, and 638.01 ha maintained their water classification throughout the period. With the MapBiomas images, 1,119.81 ha were classified as non-water, 2,818.74 ha were converted to water, and 794.04 ha remained water during the period evaluated.

Among the most prominent changes was an increase in water accumulation in the southwestern portion of the study area, corresponding to the region of the Serrinha II reservoir,

Table 3. Statistical parameters of temporal trend tests (1990-2020) for NDWI, MNDWI, and MapBiomas.

Statistics	NDWI	MNDWI	MapBiomas	MNDWI Dry	MNDWI Rainy
Kendall's tau (τ)	0.141[ns]	0.048[ns]	0.084[ns]	-0.030[ns]	0.132[ns**]
Sen's Slope (β)	29,052[ns]	8,648[ns]	19,347[ns]	-4,273[ns]	25,600[ns]

Significance codes: **5%; [ns]not significant.
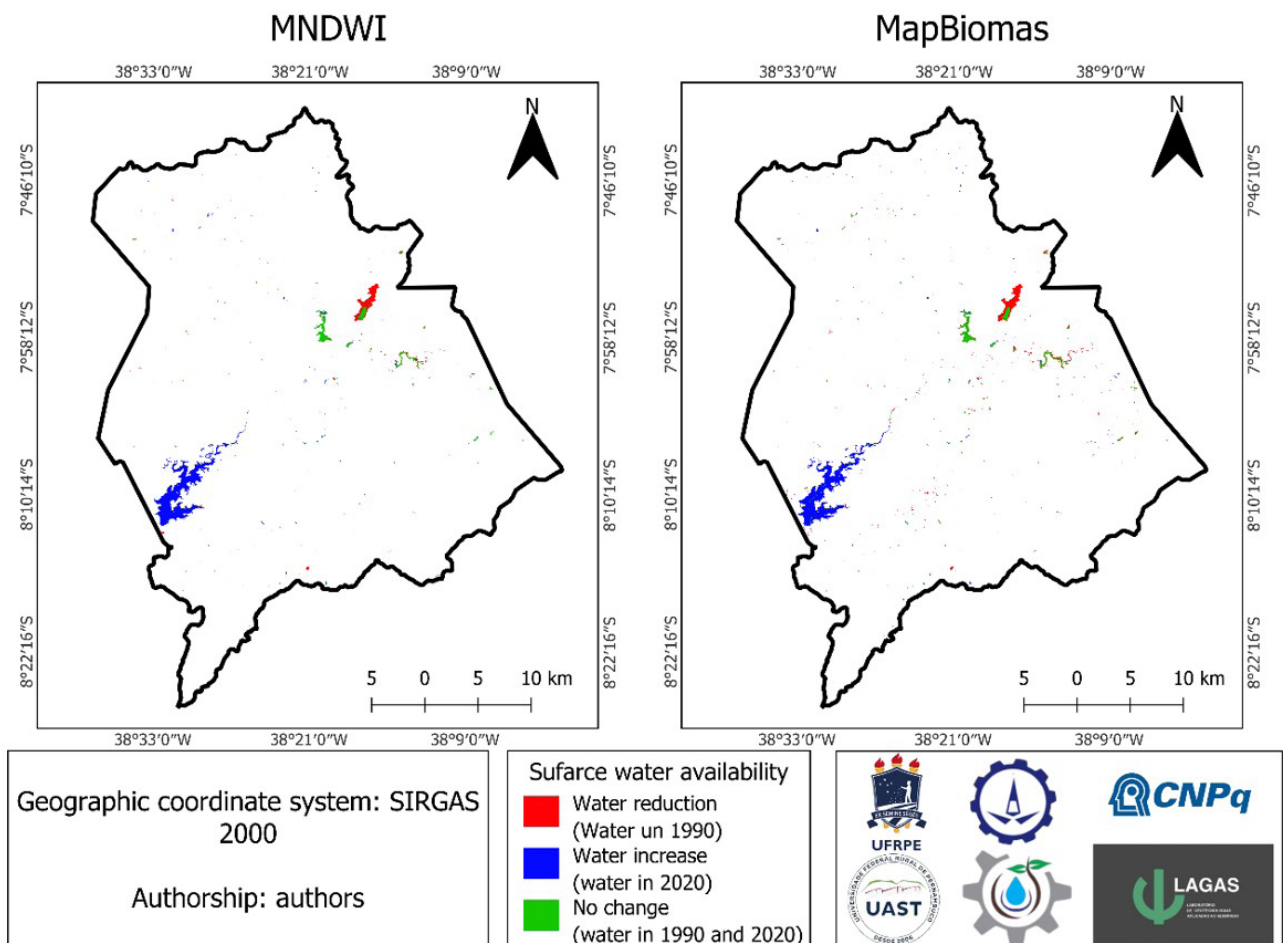
Figure 6. Transition of surface water from MNDWI and MapBiomas in Serra Talhada - PE (1990 and 2020).

where construction was completed in 1996. Simultaneously, surface water was significantly reduced in the Saco reservoir, located in the central-eastern region. Additionally, there was a varied distribution of changes, albeit with limited spatial coverage, indicating the possible formation of small reservoirs or areas of water accumulation.

Surface water reservoir density

It is observed in Figure 7 the concentration of surface water reservoirs, integrating the MNDWI and MapBiomas data for 1990 and 2020. The objective was to highlight locations with small water reservoirs in the study area. The images classified by MNDWI and MapBiomas were vectorized, followed by removing polygons classified as zero (0), corresponding to no-water areas. The centroids of the polygons were then extracted, and the layers of points obtained from the MNDWI and MapBiomas classifications were combined.

Combining MNDWI and MapBiomas was necessary due to their complementarity; MNDWI can capture pixels that MapBiomas does not detect and vice versa. This approach simplifies the identification of reservoirs, indicating that regions with more intense colors represent a higher concentration of water reservoirs. Areas with a reddish color tone have the greatest number of water reservoirs.

Can be seen in Figure 7, that in 1990, the concentration of reservoirs along the Pajeú River was higher due to the river's intermittent nature, which favors the formation of small reservoirs. The highest concentrations of reservoirs were observed upstream of the Cachoeira and Jazigo dams, located in the northeastern region of the map (Figure 1).

In 2020, the concentration of reservoirs increased, primarily due to the construction of small reservoirs, especially in the northern and southern sectors. However, a decrease in small reservoirs was observed in the vicinity of the Cachoeira and Jazigo dams, while a greater concentration of these reservoirs began to occur upstream of the Serrinha II dam.

DISCUSSIONS

A comparison was conducted using data from the MapBiomas Water collection to assess the effectiveness of the proposed method for identifying water surfaces in the semi-arid region. This database is widely recognized in the literature for using the Spectral Mixture Analysis technique, resulting in robust and consistent classifications (Souza Junior et al., 2025). However, it presents limitations regarding temporal resolution, as data are only available at annual and monthly scales and are restricted to 2023, at least the current collection.
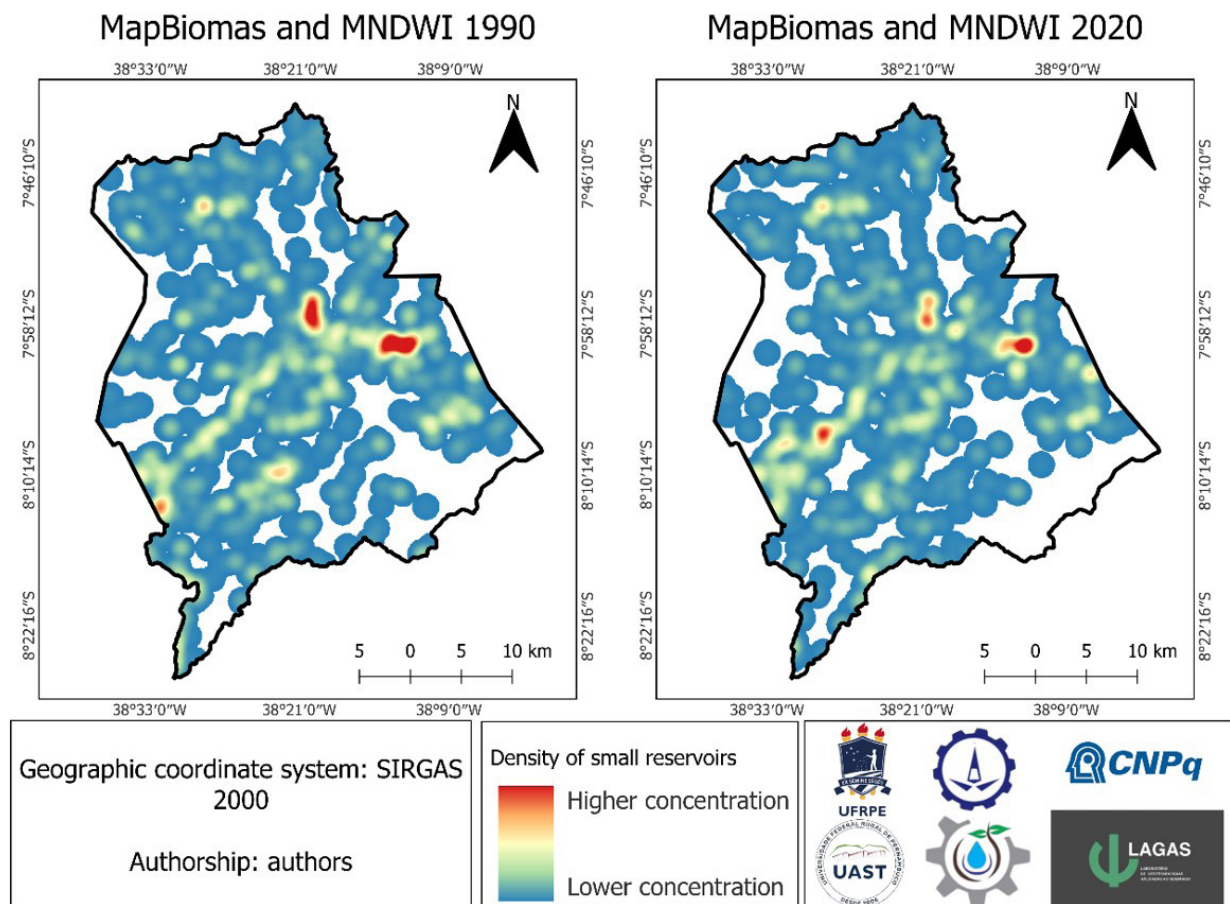
Figure 7. Density of surface water reservoirs in Serra Talhada, PE (1990 and 2020).

These constraints limit its applicability in recent analyses or studies focused on specific seasonal events. Therefore, using spectral indices such as NDWI and MNDWI, with a simple classification threshold (values greater than zero), has proved a viable and effective alternative, providing results compatible with more complex methods. Previous studies, including Lourenço et al. (2021), corroborate these indices' capacity to represent water bodies accurately. The approach adopted in this study serves as a complementary tool to consolidated databases like MapBiomas and as a potential substitute in situations where temporal or seasonal resolution is required.

The findings highlight MNDWI's superior ability to detect surface water, primarily due to the stronger spectral response of the SWIR band compared to the NIR band. This enhanced performance has been emphasized by Amiri, Seyed, and Mahmoodi (2022) in their analysis of MNDWI and NDWI on Lake Haramaya's surface in the eastern highlands of Ethiopia. An additional advantage of the MNDWI lies in the use of a zero threshold to differentiate classes, which contributes to improved water classification accuracy (Nascimento et al., 2019).

Anjos Carvalho et al. (2023) anticipated NDWI's good performance, highlighting its classification capacity comparable to MapBiomas and high conformity in reservoir areas. Nevertheless, MNDWI consistently outperformed NDWI due to its enhanced spectral sensitivity in the mid-infrared region (Nascimento et al., 2019). Supporting this observation, Xu (2006) has shown that MNDWI images offer more detail than NDWI images, particularly for detecting subtle water features, such as those in the center of Bayi Lake, better visualized with MNDWI.

The inter-annual variability of surface water areas, illustrated in Figure 5, is intrinsically linked to the region's temporal and spatial variations in rainfall (Figure 3). Climate change, with projected increases in temperature, could intensify the temporal and spatial irregularity of rainfall, affecting the distribution of water in the semi-arid region (Angelotti et al., 2012). Studies such as those by Santos Junqueira et al. (2020), Alcântara et al. (2021), and Bezerra et al. (2021) suggest changes in rainfall distribution patterns in the northeast region, especially in the semi-arid region, which may impact the availability of surface water resources in the study area.

According to Sobral et al. (2019), starting in the 1980s, there was a change in precipitation patterns, with dry years becoming more evident, indicating a possible climatic variation in the precipitation pattern in the Pernambuco backlands region. This variation became even more noticeable from the 1990s onward, as observations show that between 1990 and 2003, only dry years occurred, with no positive precipitation index or wet/rainy years recorded. The same study states that from the 2000s, four wet years were observed; however, the intensity classification remained within normal levels, without any "Very Wet" or "Extremely Wet" years.

According to observations by Afonso & Chou (2023), in the Sobradinho Lake located in northeastern Brazil, the semiarid region experienced twenty normal years, four wet years, six dry years, and one year (1993) classified as extremely dry. Also, 1993 and 2015 were characterized as drought years, associated with weak and strong El Niño episodes, respectively. In contrast, 2000 was considered an extremely wet year and was linked to a La Niña event.

The results presented in Figure 5 indicate a water retention potential of approximately 5,000 hectares in the municipality, with 40% corresponding to the Serrinha II reservoir, as highlighted in Figure 6 and in the study by Anjos Carvalho et al. (2023), which identified the reservoir's water mirror area at around 2,000 hectares in mid-2012, according to França et al. (2019), the Jazigo and Serrinha reservoirs are large and exert a significant influence on water flow. Figure 7 also indicates changes in local water classes, possibly corresponding to small reservoirs. According to Nascimento et al. (2019), these small reservoirs are essential for neighboring communities, playing a vital role in various subsistence activities.

During the drought in the region, between 2012 and 2017 (Bezerra et al., 2018; Costa et al., 2021), there was a significant reduction in the surface water area to around 1,000 hectares annually (Figure 5). This represents an 80% drop in the municipality's total storage capacity. Sousa et al. (2021) pointed out that reservoirs in the semi-arid region are highly affected by climatic seasonality, resulting in variations in water levels. Therefore, constructing reservoirs without proper planning, especially in large areas exposed to solar radiation, does not guarantee water availability during drought.

Due to the irregular rainfall characteristics, high temperature, and low annual temperature range, with rainfall distribution ranging from 200 to 800 mm per year, reservoirs are vulnerable to climatic elements, losing water significantly through evaporation. It is, therefore, essential to consider implementing different water management structures, especially for rural communities. The application of water collection and storage technologies, such as cisterns and underground dams, can be an effective intervention to control water losses, strengthen agricultural production, and mitigate the food insecurity of these populations during periods of drought (Gebru et al., 2021; Fagundes et al., 2020).

CONCLUSIONS

This study investigated the dynamics of surface water in the municipality of Serra Talhada between 1990 and 2020, aiming to identify simple and effective methods for identifying water surfaces using remote sensing products and performing time trend tests in different compartments of the historical series, with an emphasis on the dry and rainy periods, to understand the region's standard behaviors.

The performance evaluation of the water indices highlighted the superiority of MNDWI over NDWI, underscoring the importance of the mid-infrared spectral characteristics for more accurate water surface identification.

The time trend tests showed no significant difference over the evaluation period, whether annually, during dry, or rainy periods. However, the analysis revealed an annual and seasonal variation in water areas influenced by the rainfall pattern in northeastern Brazil. This highlighted the importance of understanding the impacts of these variations on water resources availability. Identifying small local reservoirs reinforced their relevance to communities, especially during drought.

The significant reduction in surface water area during the dry season between 2012 and 2017 demonstrated the

vulnerability of reservoirs in the semi-arid region to seasonal climate variations. During this period, the surface water area was reduced by approximately 80%, from around 5,000 hectares during the municipality's wettest period to around 1,000 hectares during the driest period. This scenario emphasizes the need to implement water harvesting and storage technologies as a crucial intervention to mitigate water losses, strengthen agricultural production, and address the challenges related to food insecurity in rural communities.

This study contributes to water management in semi-arid regions, providing a basis for developing strategies and public policies for conserving and using water resources. Further research is essential to improve monitoring and ensure communities' resilience in the face of climate change.

DATA AVAILABILITY STATEMENT

Research data is only available upon request.

REFERENCES

Afonso, E. O., & Chou, S. C. (2023). Modeling the effects of local atmospheric conditions on the thermodynamics of Sobradinho Lake, Northeast Brazil. *Climate*, *11*(10), 208. http://doi.org/10.3390/cli11100208.

Alcântara, L. R. P., Coutinho, A. P., Santos Neto, S. M., Cunha Rabelo, A. E. C. G., & Antonino, A. C. D. (2021). Modeling of the hydrological processes in Caatinga and Pasture areas in the Brazilian semi-arid. *Water*, *13*(13), 1877. http://doi.org/10.3390/w13131877.

Alvares, C. A., Stape, J. L., Sentelhas, P. C., Moraes Gonçalves, J. L., & Sparovek, G. (2013). Köppen's climate classification map for Brazil. *Meteorologische Zeitschrift*, *22*(6), 711-728. http://doi.org/10.1127/0941-2948/2013/0507.

Amani, M., Ghorbanian, A., Ahmadi, S., Kakooei, M., Moghimi, A., Mirmazloumi, S. M., Moghaddam, S. H. A., Mahdavi, S., Ghahremanloo, M., Parsian, S., Wu, Q., & Brisco, B. (2020). Google Earth Engine cloud computing platform for remote sensing big data applications: a comprehensive review. *IEEE Journal of Selected Topics in Applied Earth Observations and Remote Sensing*, *13*, 5326-5350. http://doi.org/10.1109/JSTARS.2020.3021052.

Amiri, K., Seyed, H., & Mahmoodi, F. (2022). Study and monitoring of wetland area changes and its impact on wetland surface temperature using NDWI, MNDWI, and AWEI indices (Case study: Hur al-Azim and Shadegan Wetlands). *Journal of Irrigation Sciences and Engineering*, *44*, 59-74. http://doi.org/10.22055/jise.2020.31854.1898.

Angelotti, F., Fernandes Júnior, P. I., & Sá, I. B. (2012). Mudanças climáticas no semiárido brasileiro: medidas de mitigação e adaptação. *Revista Brasileira de Geografia Física*, *4*(6), 1097-1111. http://doi.org/10.26848/rbgf.v4i6.232763.

Anjos Carvalho, W., Cezar Bezerra, A., & Alba, E. (2023). Comparison between three methods to monitor reservoir extension in the Brazilian semi-arid region. *Anuario Instituto de Geociencias*, *46*, 43387. http://doi.org/10.11137/1982-3908_2023_46_43387.

Araujo, H. F. P., Canassa, N. F., Machado, C. C. C., & Tabarelli, M. (2023). Human disturbance is the major driver of vegetation changes in the Caatinga dry forest region. *Scientific Reports*, *13*(1), 18440. http://doi.org/10.1038/s41598-023-45571-9.

Arnold, T., & Emerson, J. (2011). Nonparametric goodness-of-fit tests for discrete null distributions. *The R Journal*, *3*(2), 34. http://doi.org/10.32614/RJ-2011-016.

Barros, M. F., Ribeiro, E. M. S., Vanderlei, R. S., de Paula, A. S., Silva, A. B., Wirth, R., Cianciaruso, M. V., & Tabarelli, M. (2021). Resprouting drives successional pathways and the resilience of Caatinga dry forest in human-modified landscapes. *Forest Ecology and Management*, *482*, 118881. http://doi.org/10.1016/j.foreco.2020.118881.

Bezerra, A. C., Silva, J. D., Costa, S. D., Silva, A. D., & Aburqueque, G. D. (2018). Space analysis on the Cachoeira II-Pe reservoir margins with vegetation indexes. *Amazonian Journal of Plant Research*, *2*(4), 247-253. http://doi.org/10.26545/ajpr.2018.b00031x.

Bezerra, A. C., Costa, S. A. T., Silva, J. L. B., Araújo, A. M. Q., Moura, G. B. A., Lopes, P. M. O., & Nascimento, C. R. (2021). Annual rainfall in Pernambuco, Brazil: regionalities, regimes, and time trends. *Revista Brasileira de Meteorologia*, *36*(3), 403-414. http://doi.org/10.1590/0102-77863630129.

Brasil. Serviço Público Federal. Casa Civil. (2017). *Relatório de Análise de Mercado de Terras – RAMT*. Brasília. Retrieved in 2024, July 16, from https://www.gov.br/incra/pt-br/assuntos/governanca-fundiaria/relatorio-de-analise-de-mercados-de-terras/ramt_sr28_2017.pdf

Chen, J., Chen, S., Fu, R., Li, D., Jiang, H., Wang, C., Peng, Y., Jia, K., & Hicks, B. J. (2022). Remote sensing big data for water environment monitoring: current status, challenges, and future prospects. *Earth's Future*, *10*(2), e2021EF002289. http://doi.org/10.1029/2021EF002289.

Congedo, L. (2021). Semi-Automatic classification plugin: a Python tool for the download and processing of remote sensing images in QGIS. *Journal of Open Source Software*, *6*(64), 3172. http://doi.org/10.21105/joss.03172.

Congedo, L. (2024). *Semi-automatic classification plugin documentation, release 8.1.3.1*. San Francisco, CA: GitHub. Retrieved in 2024, November 23, from https://app.readthedocs.org/projects/semiautomaticclassificationmanual-v5-fa/downloads/pdf/latest/

Costa, S., Bezerra, A., Araújo, A., Silva, M., Cruz Neto, J., Alves, R., & Souza, L. (2021). Dinâmica espaço-temporal das anomalias de precipitação em uma região semiárida, Nordeste do Brasil. *Revista de Gestão de Água da América Latina*, *18*, e14. http://doi.org/10.21168/rega.v18e14.

Gouveia, J. R. F., Nascimento, C. R., da Silva, H. C., Moura, G. B. de A., & Lopes, P. M. O. (2024). Influência de eventos climáticos extremos na ocorrência de queimadas e no poder de regeneração vegetal. *Revista Brasileira de Geografia Física*, *17*(2), 1098-1113. http://doi.org/10.26848/rbgf.v17.2.p1098-1113.

Deus, D., & Gloaguen, R. (2013). Remote sensing analysis of lake dynamics in semi-arid regions: implication for water resource management. Lake Manyara, east African rift, northern Tanzania. *Water*, *5*(2), 698-727. http://doi.org/10.3390/w5020698.

Diniz, C., Cortinhas, L., Pinheiro, M. L., Sadeck, L., Fernandes Filho, A., Baumann, L. R. F., Adami, M., & Souza-Filho, P. W. M. (2021). A large-scale deep-learning approach for multi-temporal aqua and salt-culture mapping. *Remote Sensing*, *13*(8), 1415. http://doi.org/10.3390/rs13081415.

Ebrahimi-Khusfi, Z., Ghazavi, R., & Zarei, M. (2020). The effect of climate changes on the wetland moisture variations and its correlation with sand-dust events in a semiarid environment, Northwestern Iran. *Photonirvachak (Dehra Dun)*, *48*(12), 1797-1808. http://doi.org/10.1007/s12524-020-01203-7.

Fagundes, A. A., Silva, T. C., Voci, S. M., Dos Santos, F., Barbosa, K. B. F., & Corrêa, A. M. S. (2020). Food and nutritional security of semi-arid farm families benefiting from rainwater collection equipment in Brazil. *PLoS One*, *15*(7), e0234974. http://doi.org/10.1371/journal.pone.0234974.

Ferreira, V. S. (2022). *Mapeamento do uso e cobertura do solo de uma região do Pontal do Paranapanema para estimativa da produção de biocombustível* (Trabalho de conclusão de curso). Universidade Estadual Paulista, Rosana, SP.

França, L. M. A., Diaz, C. C. F., Reis, J. V., Costa, V. S. O., & Galvíncio, J. D. (2019). Efeitos da precipitação na vazão da bacia hidrográficado rio Pajeú-PE. *Revista Brasileira de Geografia Física*, *12*(6), 2377-2391. http://doi.org/10.26848/rbgf.v12.6.p2377-2391.

Gebru, T. A., Brhane, G. K., & Gebremedhin, Y. G. (2021). Contributions of water harvesting technologies intervention in arid and semi-arid regions of Ethiopia, in ensuring households' food security, Tigray in focus. *Journal of Arid Environments*, *185*, 104373. http://doi.org/10.1016/j.jaridenv.2020.104373.

Gorelick, N., Hancher, M., Dixon, M., Ilyushchenko, S., Thau, D., & Moore, R. (2017). Google Earth Engine: planetary-scale geospatial analysis for everyone. *Remote Sensing of Environment*, *202*, 18-27. http://doi.org/10.1016/j.rse.2017.06.031.

Gxokwe, S., Dube, T., & Mazvimavi, D. (2022). Leveraging Google Earth Engine platform to characterize and map small seasonal wetlands in the semi-arid environments of South Africa. *The Science of the Total Environment*, *803*, 150139. http://doi.org/10.1016/j.scitotenv.2021.150139.

Instituto Nacional de Meteorologia – INMET. (2024). Retrieved in 2024, November 23, from https://portal.inmet.gov.br/

Leroux, L., Congedo, L., Bellón, B., Gaetano, R., & Bégué, A. (2018). Land cover mapping using sentinel-2 images and the semi-automatic classification plugin: a northern Burkina Faso case study. In N. Baghdadi, C. Mallet, & M. Zribi (Eds.), *QGIS and applications in agriculture and forest* (pp. 119-151). Hoboken: John Wiley & Sons. http://doi.org/10.1002/9781119457107.ch4.

Lins, F. A. C., Silva, J. L. B., Moura, G. B. D. A., Ortiz, P. F. S., Oliveira, J. D. A., & Alves, M. V. C. (2018). Quantile technique to precipitation, rainfall anomaly index and biophysical parameters by remote sensing in Serra Talhada, Pernambuco. *Journal of Hyperspectral Remote Sensing*, *7*(6), 334-344. http://doi.org/10.29150/jhrs.v7.6.p334-344.

Lourenço, V. R., Carvalho, A. A., Almeida, G. D. C., & Assunção Montenegro, A. A. (2021). Comparison of the area of water masses in a hydrographic basin using spectral indices and MapBioma's classification. *Journal of Hyperspectral Remote Sensing*, *11*(4), 196-203.

MapBiomas. (2024). *Plataforma MapBiomas Brasil*. Retrieved in 2024, September 18, from http://plataforma.brasil.mapbiomas.org/

Marengo, J. A., Alves, L. M., Beserra, E. A., & Lacerda, F. F. (2011). Variabilidade e mudanças climáticas no semiárido brasileiro. In Instituto Nacional do Semiárido (Ed.), *Recursos hídricos em regiões áridas e semiáridas* (Vol. 1, pp. 385-422). Brasília: INSA. Retrieved in 2024, September 18, from https://repositorio.mcti.gov.br/handle/mctic/5720

Mashala, M. J., Dube, T., Mudereri, B. T., Ayisi, K. K., & Ramudzuli, M. R. (2023). A systematic review on advancements in remote sensing for assessing and monitoring land use and land cover changes impacts on surface water resources in semi-arid tropical environments. *Remote Sensing*, *15*(16), 3926. http://doi.org/10.3390/rs15163926.

McFeeters, S. K. (1996). The use of the Normalized Difference Water Index (NDWI) in the delineation of open water features. *International Journal of Remote Sensing*, *17*(7), 1425-1432. http://doi.org/10.1080/01431169608948714.

Medeiros, C. J. F., & Costa, J. A. F. (2008). Uma comparação empírica de métodos de redução de dimensionalidade aplicados a visualização de dados. *Learning and Nonlinear Models*, *6*(2), 81-110. http://doi.org/10.21528/LNLM-vol6-no2-art1.

Mortatti, J., Bortoletto Junior, M. J., Milde, L. C. E., & Probst, J. L. (2004). Hidrologia dos rios Tietê e Piracicaba: séries temporais de vazão e hidrogramas de cheia. *Revista de Ciência & Tecnologia*, *12*(23), 55-67. Retrieved in 2024, September 18, from https://silo.tips/download/hidrologia-dos-rios-tiete-e-piracicaba-series-temporais-de-vazao-e-hidrogramas-d#google_vignette

Nascimento, E. F., Oliveira, L. M. M., Lima, J. F., Montanhas Farias, A. A., & Silva, J. G. (2019, April). Comparação de índices de água na identificação de corpo hídrico por sensoriamento remoto. In *Anais do XIX Simpósio Brasileiro de Sensoriamento Remoto*, Santos, SP. Retrieved in 2024, September 18, from https://proceedings.science/

sbsr-2019/trabalhos/comparacao-de-indices-de-agua-na-identificacao-de-corpo-hidrico-por-sensoriament?lang=pt-br

Pandey, V., Pandey, P. K., Chakma, B., & Ranjan, P. (2023). Influence of short-and long-term persistence on identification of rainfall temporal trends using different versions of the Mann-Kendall test in Mizoram, Northeast India. *Environmental Science and Pollution Research International*, *31*(7), 10359-10378. http://doi.org/10.1007/s11356-023-29436-2.

Patakamuri, S. K., & O'Brien, N. (2023). *modifiedmk: Modified Versions of Mann-Kendall and Spearman's Rho Trend Tests. Version 1.6.0*. Vienna: R Foundation for Statistical Computing. Retrieved in 2024, September 18, from https://CRAN.R-project.org/package=modifiedmk

Pilz, T., Delgado, J. M., Voss, S., Vormoor, K., Francke, T., Costa, A. C., Martins, E., & Bronstert, A. (2019). Seasonal drought prediction for semiarid northeast Brazil: what is the added value of a process-based hydrological model? *Hydrology and Earth System Sciences*, *23*(4), 1951-1971. http://doi.org/10.5194/hess-23-1951-2019.

Pohlert, T. (2023). *trend: Non-Parametric Trend Tests and Change-Point Detection. Version 1.1.6*. Vienna: R Foundation for Statistical Computing. Retrieved in 2024, September 18, from https://CRAN.R-project.org/package=trend

Rodrigues, E. L., Sousa, F. A. S., & Lopes, F. C. R. (2022). Análise da variabilidade dos períodos secos e chuvosos da precipitação pluvial no estado da Paraíba utilizando o Índice Padronizado de Precipitação (IPP). *Revista Brasileira de Geografia Física*, *15*(5), 2544-2581. http://doi.org/10.26848/rbgf.v15.5.p2544-2581.

Rundquist, D., Lawson, M., Queen, L., & Cerveny, R. (1987). The relationship between the timing of summer-season rainfall events and lake-surface area. *Journal of the American Water Resources Association*, *23*(3), 493-508. http://doi.org/10.1111/j.1752-1688.1987.tb00828.x.

Santos Junqueira, H., Moreira Fernandes de Almeida, L., Santos de Souza, T., & Santos Nascimento, P. (2020). Análise da variação sazonal e de tendências na precipitação pluviométrica no município de Juazeiro-BA. *Revista Brasileira de Geografia Física*, *13*(6), 2641-2649. http://doi.org/10.26848/rbgf.v13.6.p2641-2649.

Silva, V. P. R., Correia, A. A., & Coelho, M. S. (1998). Análise de tendência das séries de precipitação pluvial do nordeste do Brasil. *Revista Brasileira de Engenharia Agrícola e Ambiental*, *2*(1), 111-114. http://doi.org/10.1590/1807-1929/agriambi.v2n1p111-114.

Silverman, B. W. (1978). Weak and strong uniform consistency of the kernel estimate of a density function and its derivatives. *Annals of Statistics*, *6*(1), 177-184. http://doi.org/10.1214/aos/1176344076.

Sobral, M. C., Assis, J. M. O., Oliveira, C. R., Silva, G. M. N., Morais, M., & Carvalho, R. M. C. (2019). Impacto das mudanças climáticas nos recursoshídricos no submédio da bacia hidrográfica do Rio São Francisco - Brasil. *Revista Eletrônicado PRODEMA*, *12*(3), 95-106.

Sousa, K. A., Espindola, G. M., & Silva, C. E. (2021). Análise de atributos limnológicos em reservatórios do semiárido nordestino.

Revista Brasileira de Geografia Física, *14*(1), 357-371. http://doi.org/10.26848/rbgf.v14.1.p357-371.

Sousa, A. A., Lira, M. A. T., Oliveira, U. C., & Mendes Júnior, C. A. (2022). Análise multitemporal do espelho d'água do açude Jaburu I por meio de ferramentas de sensoriamento remoto nos anos de 2013 a 2020. *Revista Brasileira de Meteorologia*, *37*(2), 233-241. http://doi.org/10.1590/0102-77863720026.

Souza Junior, C. M., Kirchhoff, F. T., Oliveira, B. C., Ribeiro, J. G., & Sales, M. H. (2019). Long-term annual surface water change in the Brazilian Amazon Biome: potential links with deforestation, infrastructure development and climate change. *Water*, *11*(3), 566. http://doi.org/10.3390/w11030566.

Souza Junior, C. M., Schirmbeck, J., Ferreira Gama, B., Medeiros Brandão, I., Ribeiro Ferreira, J. G., Costa, D., Vasconcelos, R., Galano, S., Franca-Rocha, W., Vélez Martin, E., Wolfarth Schirmbeck, L., Pereira, J. J., Conciani, D., Reis Rosa, E., Dias, M., Neto, H. S. A., Silva, I. M. C., dos Reis Azevedo, R., Shimbo, J., Rosa, M., & Azevedo, T. (2025). *MapBiomas Water Brazil General "Handbook" - Algorithm Theoretical Basis Document (ATBD) - Collection 3 (Version 1). MapBiomas Data, V1*. Brasília: MapBiomas. http://doi.org/10.58053/MapBiomas/NH82QZ.

Tulbure, M. G., Broich, M., Stehman, S. V., & Kommareddy, A. (2016). Surface water extent dynamics from three decades of seasonally continuous Landsat time series at subcontinental scale in a semi-arid region. *Remote Sensing of Environment*, *178*, 142-157. http://doi.org/10.1016/j.rse.2016.02.034.

Wickham, H. (2016). *ggplot2: elegant graphics for data analysis*. New York: Springer-Verlag. http://doi.org/10.1007/978-3-319-24277-4.

Xu, H. (2002). Spatial expansion of urban/town in Fuqing of China and its driving force analysis. *Remote Sensing Technology and Application*, *17*, 86-92.

Xu, H. (2006). Modification of normalised difference water index (NDWI) to enhance open water features in remotely sensed imagery. *International Journal of Remote Sensing*, *27*(14), 3025-3033. http://doi.org/10.1080/01431160600589179.

Yu, G., Liu, D., Zhou, H., Zen, L., Zhong, Y., & Zhang, C. (1998). Automated identification of swamp land incorporating Landsat imaging and GIS data. *Hyperspectral Remote Sensing and Application*, *3502*, 267 http://doi.org/10.1117/12.317801.

Authors contributions

Geovane de Andrade Silva: Execution of data collection, methodology, statistical analysis, preparation of figures and tables, and development of the manuscript.

Érick Mateus de Souza Freire: Involvement in data collection, content review, and critical analysis of the issue under study.

Francisco Gustavo da Silva: Contribution to the preparation of figures and tables, methodology, content review, and analysis of the presented problem.

José Raliuson Inácio Silva: Participation in statistical analysis, methodology, content review, and exploration of the central theme.

Antônio Henrique Cardoso do Nascimento: Contribution to the methodology, preparation of figures and tables, and analysis of the problem addressed in the study.

Elisiane Alba: Collaboration in the methodology and examination of the issue raised in the research.

Araci Farias Silva: Contribution to the methodology, evaluation of the discussed topic, and content review.

Alan Cézar Bezerra: Collaboration in the exploration of the central theme, methodology, statistical analysis, figure preparation, and content review.